

# Regulation of Microtubule Dynamics in 3T3 Fibroblasts by Rho Family GTPases

Ilya Grigoriev,<sup>1\*</sup> Gary Borisy,<sup>2</sup> and Ivan Vorobjev<sup>1,3</sup>

<sup>1</sup>*Cell Biology and Histology Department, Moscow State University Biological Faculty, Vorobjevi Gory, Moscow 119992, Russia*

<sup>2</sup>*Cell and Molecular Biology Department, Northwestern University Medical School, Chicago, Illinois 60611*

<sup>3</sup>*Cell Motility Lab, Belozersky Institute, Moscow State University, Vorobjevi Gory, Moscow 119992, Russia*

To get insight into the action of Rho GTPases on the microtubule system we investigated the effects of Cdc42, Rac1, and RhoA on the dynamics of microtubules in Swiss 3T3 fibroblasts. In control cells microtubule ends were dynamic: plus ends frequently switched between growth, shortening and pauses; the growth phase predominated over shortening. Free minus ends of microtubules depolymerized rapidly and never grew. Free microtubules were short-lived, and the microtubule network was organized into a radial array. In serum-starved cells microtubule ends became more stable: although plus ends still transited between growth and shortening, polymerization and depolymerization excursions became shorter and balanced each other. Microtubule minus ends were also stabilized. Consequently lifespan of free microtubules increased and microtubule array changed its radial pattern into a random one. Activation of Cdc42 and Rac1 in serum-starved cells promoted dynamic behavior of microtubule plus and minus ends, while inhibition of these GTPases in serum-grown cells suppressed microtubule dynamics and mimicked all effects of serum starvation. Activation of RhoA in serum-grown cells had effects similar to Cdc42/Rac1 inactivation: it suppressed the dynamics of plus and minus ends, reduced the length of growth and shrinking episodes, and disrupted the radial organization of microtubules. However, in contrast to Cdc42 and Rac1 inactivation, active RhoA had no effect on the balance between microtubule growth and shortening. We conclude that Cdc42 and Rac1 have similar stimulating effects on microtubule dynamics while RhoA acts in an opposite way. *Cell Motil. Cytoskeleton* 63:29–40, 2006. © 2005 Wiley-Liss, Inc.

**Key words:** Cdc42; Rac1; RhoA; dynamic instability; microtubule plus ends; microtubule minus ends

## INTRODUCTION

Microtubules (MTs) are essential for polarization and motility of many animal cells. In fibroblast-like cells continuous flow of different cargoes along MTs supports extension of the leading edge [Bergmann et al., 1983; Wacker et al., 1997; Hirschberg et al., 1998; Lippincott-Schwartz et al., 2000; Schmoranzler et al., 2003]. Meanwhile MTs themselves are dynamic—their plus ends undergo alternating phases of growth, shortening and pauses, a phenomenon called dynamic instability (see review Desai and Mitchison, 1997). Dynamic instability

The supplemental materials described in this article can be found at <http://www.interscience.wiley.com/jpages/0886-1544/suppmat>

Contract grant sponsor: CRDF; Contract grant number: RBI-2025; Contract grant sponsor: FIRCA; Contract grant number: TW-00748; Contract grant sponsor: RFBR; Contract grant number: 05-04-49847.

\*Correspondence to: Ilya Grigoriev, Department of Cell Biology and Genetics, Erasmus Medical Center, PO Box 1738, 3000DR Rotterdam, The Netherlands. E-mail: [i.grigorev@erasmusmc.nl](mailto:i.grigorev@erasmusmc.nl)

Received 22 August 2005; Accepted 28 October 2005

Published online 16 December 2005 in Wiley InterScience ([www.interscience.wiley.com](http://www.interscience.wiley.com)).

DOI: 10.1002/cm.20107

is critical for cell motility—stabilization of MTs by different drugs inhibits cell migration [Liao et al., 1995; Mikhailov and Gundersen, 1998; Grigoriev et al., 1999]. One of the underlying mechanisms is that dynamic interactions of MTs with focal adhesions are important for the regulation of cell attachment and protrusion [Kaverina et al., 1998, 1999, 2000]. But relatively little is known about the mechanism(s) by which MT dynamics can be regulated. Keeping in mind that MTs interact in many ways with the actin cytoskeleton it is worthwhile to assume that regulation of MT dynamics occurs along with the remodeling of the actin cytoskeleton.

Key regulators of actin cytoskeleton are small Rho GTPases. They regulate actin remodeling in response to external signals, such as growth factors, cytokines, or neurotransmitters [Ridley et al., 1992; Ridley and Hall, 1992; Kozma et al., 1995; Nobes and Hall, 1995; 1999] and also are supposed to be involved in the cross-talk between actin and MTs. MT growth activates Rac1 protein, which in turn induces actin polymerization and lamellipodia formation [Waterman-Storer et al., 1999]. MT depolymerization activates RhoA protein, which induces cell contraction [Liu et al., 1998]. RhoA protein, in turn, stabilizes MTs through its effector mDia [Cook et al., 1998; Palazzo et al., 2001; Wen et al., 2004]. Cdc42 and Rac1 are supposed to destabilize MT ends by switching MT stabilizer X-PAK5 from MT to actin [Cau et al., 2001], allowing MTs to switch between growth and shortening. Besides this, Cdc42 and Rac1 activate p65PAK kinase that inhibits catastrophe promoting factor stathmin [Daub et al., 2001] and therefore stimulate MT growth. Rac1 also regulates MT stabilizer CLASP in cell lamella [Wittmann and Waterman-Storer, 2005]. Thus Cdc42 and Rac1 may facilitate MTs growth into lamella and their subsequent capture.

Multiple studies deal with the regulation of MT dynamics near the cell cortex [Kaverina et al., 1998, 1999, 2000; Fukata et al., 2002; Komarova et al., 2002a, 2002b; Mimori-Kiyosue et al., 2005; Wittmann and Waterman-Storer, 2005]. The studies of MT stabilization by RhoA [Cook et al., 1998; Palazzo et al., 2001; Wen et al., 2004], based on monitoring of the formation of deetyrosinated MTs, demonstrated that such stable MTs contact the cell margin. The majority of these observations did not address an important issue—how are the dynamic properties of *free* MT ends regulated (particularly by Rho-proteins)? How do MT ends arrive at the cell edge, where they start to be controlled by the regulators listed earlier? Another question deals with the behavior of the minus ends. In fibroblast-like cells free minus ends are considered to be continuously disassembling, while in epithelial cells they are rather stable [Vorobjev et al., 1997]. It is still unknown whether behavior of the minus ends (switching between pause and shortening) could be

regulated. Stabilization of the minus ends in CHO cells by making cell–cell contacts was demonstrated [Chausovsky et al., 2000]; however, the dynamics of the minus ends under these conditions was not examined.

For answering the questions about the regulation of the dynamics of free MT ends by Rho proteins, we directly observed the behavior of MT ends in living cells upon activation or inhibition of three Rho-family members—Cdc42, Rac1, and RhoA. Plus and minus ends of MTs were followed in internal lamella regions and parameters of dynamic instability were calculated. Plus ends were also analyzed in the framework of the random walk approach, which was already successfully applied to quantify the behavior of the MT population [Vorobjev et al., 1997; Vorobjev et al., 1999; Komarova et al., 2002a]. This approach (which is explained in brief below or can be found in more detail in Vorobjev et al. [1999]) uses two parameters, the diffusion coefficient and the drift coefficient to characterize the behavior of the MT end population. The diffusion coefficient is as a measure of the space covered by the excursions of growing or shrinking MT ends; in principle it can be considered as a measure of the searching reaction. The drift coefficient is a mean displacement of MT ends with time; it represents the imbalance of growth and shortening excursions over time. Using these two approaches, dynamic instability model and random walk, Cdc42 and Rac1 were found to promote dynamic instability of the plus and minus ends, while RhoA partially stabilized both plus and minus ends of MTs. Stabilization achieved by inhibition of Cdc42 or Rac1, and by activation of RhoA was similar to the effects of cultivation of cells without serum or application of nocodazole at nanomolar concentrations.

## MATERIALS AND METHODS

### Cell Culture

Swiss-3T3 fibroblasts (ATCC, Rockville, MD) were grown in Dulbecco's modified minimum essential medium (DMEM, CellGro) supplemented with 10% fetal calf serum (FCS), glucose (4.5 g/l), L-glutamine, sodium pyruvate, and penicillin/streptomycin at 37°C under 5% CO<sub>2</sub>. Cells were plated 2 days before experiments into observation chambers made by attaching a coverslip with Sylgard silicone elastomer (Dow Corning, Midland, MI) over a hole drilled in a 35-mm culture dish. After 2 days, a part of the monolayer was scratched with a razor blade, and 2 h later, cells at the edge of the experimental wound were microinjected.

### MT Visualization

Cells were microinjected by Cy3-labelled porcine brain tubulin for visualization of MTs. Cy3-labelled

tubulin was prepared as described elsewhere [Keating et al., 1997] and stored in 10- $\mu$ l aliquots in liquid nitrogen. Prior to microinjection, a 10- $\mu$ l aliquot of Cy3-tubulin was diluted with 5  $\mu$ l of PM buffer (0.1 M Pipes, 1 mM MgCl<sub>2</sub>, pH 6.9), centrifuged at 200,000g for 10 min at 4°C to remove particulate material and minimize micropipette clogging, and stored on ice until the time of injection. Cells injected with Cy3-tubulin were treated with the oxygen-depleting enzyme oxyrase (Oxyrase, Inc., Ashland, OH) to reduce photodamage and photobleaching [Mikhailov and Gundersen, 1995]. Oxyrase was added to the observation chamber at a final dilution of 2–3% (v/v) of the original stock, along with lactic acid at a final concentration of 20 mM. The oxyrase-treated dishes were then covered with a layer of mineral oil (Squibb and Sons, Princeton, NJ).

### Immunofluorescence Staining

Cells were fixed in a culture dish with glutaraldehyde (at a final concentration of 1.5%), permeabilized in 0.1% Triton X-100, rinsed in PBS (phosphate-buffered saline, pH 7.3), treated with sodium borohydrid (2% in PBS), and stained with monoclonal anti- $\beta$ -tubulin antibodies (ICN), and then with Alexa-488-conjugated anti-mouse antibodies (Molecular Probes). For actin staining Texas Red labeled phalloidin (Molecular Probes) was used.

### Imaging

Injected cells were observed on a Nikon Diaphot 300 inverted microscope equipped with a Plan  $\times$ 100, 1.25 NA objective using a rhodamine filter set. Images of 16-bit depth were collected with a CH350 cooled CCD camera (Photometrics Ltd., Tucson, AZ) driven by Metamorph imaging software (Universal Imaging Corp., Westchester, PA). The image was projected onto the CCD chip at a magnification of 0.09  $\mu$ m/pixel (11.1 pixels/ $\mu$ m). Exposure time was 0.5 s, and images were collected at 3-s intervals. Cells were kept at 37°C during observation. A typical series comprised 100 frames, covering a period of 5 min.

Sixteen-bit images were deconvolved in Metamorph software by self-written algorithm. A copy of 16-bit image (or a stack) was blurred by low pass filter. Then blurred image was subtracted from the original one. The resultant 2D-deconvolved image had uniform background where individual MTs were equally visible in all parts of the cell.

### Rho-Activator and Inhibitor Treatments and Reagents

Selective activation or inhibition of Rho proteins was performed as described by Nobes and Hall [1999]. Briefly, for activation of Cdc42, Rac1, and RhoA pro-

teins we microinjected cells with constitutively active recombinant proteins L61Cdc42-GST, L61Rac1-GST, and L63RhoA-GST, respectively (Cytoskeleton, USA) at a final needle concentration of 0.5  $\mu$ g/ml. For inactivation of Cdc42, Rac1, and RhoA proteins we microinjected dominant negative recombinant proteins N17 Cdc42-GST, N17Rac1-GST, and C3 transferase, respectively (Cytoskeleton, USA) at a final needle concentration of 0.5  $\mu$ g/ml.

The constitutively active form of human Cdc42 protein has a glutamine to leucine substitution at amino acid 61. The leucine substitution prevents GAP-stimulated GTPase activity of Cdc42, and hence the protein is always in the active, GTP-bound state. The constitutively active Rac1 and RhoA recombinant proteins had single amino acid substitution with the same effect on protein function.

The dominant negative form of human Cdc42 protein has a threonine to asparagine substitution at amino acid 17. The asparagine substitution stabilizes the GDP bound form of the protein, and hence the protein is always in the inactive state. In case of Rac1 recombinant protein there is also an amino acid substitution with the same effect on protein function. For RhoA inactivation we used C3 transferase, which is ADP-ribosyl transferase, selectively ribosylating RhoA at asparagine 41 residue. This ribosylation does not affect GTPase activity of RhoA protein, but blocks RhoA interaction with downstream effectors [Sekine et al., 1989].

For MT stabilization we used nocodazole (Sigma) at a final concentration of 100 nM.

### Quantitative Data Analysis

Analysis of MT dynamics in terms of dynamic instability was done as described by Sheldon and Wadsworth [1993]. Briefly, to quantify the behavior of individual MTs, the positions of the MT ends were followed using a mouse-driven cursor under Metamorph software (Universal Imaging Corp., Downingtown, PA). Both *X* and *Y* coordinates of the position of a given MT end in each frame were measured and logged into Excel software using dynamic data exchange protocol, and then copied and further analyzed in SigmaPlot 2001 for Windows (SPSS Inc., Chicago, IL). The phases of growth, shortening, and pause were selected; only changes > 0.5  $\mu$ m were considered growth or shortening events. The rates of growth and shortening events were determined. The frequencies of transition from one phase to another were calculated by dividing the total number of given transitions by the total time spent in this phase. The frequencies of six transitions were determined (transition from growth to pause, from growth to shortening, from shortening to growth, from shortening to pauses, from pauses to growth,

from pauses to shortening). All values given in the text are mean  $\pm$  SD unless stated differently.

Analysis of MT dynamics in terms of the random walk model was done as described by Vorobjev et al. [1999]. In brief, under the random walk approach the behavior of a MT end is considered an analogue of that for a diffusing particle. The drift value is determined as a mean displacement of MT ends with time. The diffusion coefficient is determined as mean rate of growth of the variance of displacement of MT ends with time. The mean square displacement of a MT end from its initial position was determined in 30-s time interval and linear regression plot of mean square displacement versus time was created  $x^2 = st$ . For a 1D random walk, the diffusion coefficient  $D = s/2$  [Berg, 1993]. All values given for drift and diffusion are mean  $\pm$  SEM.

## RESULTS

### Inhibition of Either Cdc42 or Rac1 and Activation of RhoA Induce Changes in the Spatial Organization of MTs

In agreement with previous studies microinjection of dominant negative Cdc42 protein induced filopodia disassembly, microinjection of dominant negative Rac1 protein caused lamellipodia disappearance and microinjection of C3 transferase (RhoA inhibitor) lead to disassembly of stress fibers (data not shown). MTs were still present after these changes in actin cytoskeleton took place. Although there was no gross effect on the spatial density of the MTs, some changes in their organization were evident under high magnification (Fig. 1). In control cells MTs were organized in a typical fibroblast-type radial array, running from the centrosome straight toward the cell margin (Fig. 1A). After microinjection of either dominant negative Cdc42 or Rac1, MTs acquired a random distribution throughout the lamella (Figs. 1B and 1C) i.e. more MTs were directed perpendicular to the cell radius or the long axis of the lamella. Inactivation of RhoA induced no visible effects on the MT pattern (Fig. 1D).

Activation of Rho GTPases was carried out in serum-starved cells. In line with previous studies, cells incubated for 2 days without serum lost filopodia and lamellipodia completely and the number of stress fibers was significantly diminished (data not shown). In serum-depleted cells MT pattern was similar to that observed in cells with inactivated Cdc42 or Rac1 (Fig. 1F). Microinjection of constitutively active Cdc42 into serum-starved cells restored filopodia activity (data not shown) and radial MT organization (Fig. 1G). Microinjection of constitutively active Rac1 into serum-starved cells restored lamellipodial activity (data not shown) as well as the radial organization of MTs (Fig. 1H). Microinjection of constitutively active RhoA lead to an increased forma-

tion of stress fibers (data not shown), and similar to inactivation of Cdc42/Rac1 in serum-grown cells, caused a somewhat increased randomization of the MT system (Fig. 1I). However, in this case many MTs became curled, while upon inactivation of Cdc42 or Rac1 they remained straight. Activation of RhoA in the presence of serum showed a more prominent effect on MT bending (Fig. 1J). MT curvature was induced by the increased centripetal flux that was visible in observations of live cells when many MTs running parallel to the cell margin were dragged toward the cell center (data not shown).

The loss of radial orientation of MTs in the lamellae could also be induced by nocodazole applied at nanomolar concentration (Fig. 1E). Thus we hypothesized that the inhibition of Cdc42 and Rac1 as well as the activation of RhoA stabilized MTs by slowing down their exchange with soluble tubulin. To test this hypothesis we measured parameters of dynamic instability of MT plus and minus ends.

### Inhibition of Cdc42 or Rac1 Alters the Parameters of Dynamic Instability of the MT Plus Ends

Swiss 3T3 fibroblasts polarized at the edge of an experimental wound were observed within 30–90 min after injection of a particular Rho protein and 5 min long time-lapse movies were recorded. To analyze dynamic instability parameters we selected MTs whose plus ends did not come closer than 3  $\mu\text{m}$  to the cell margin during the observation period. Such limitation was introduced to avoid boundary effect described earlier [Komarova et al., 2002a]. In 2D-deconvolved images (Suppl. Video Fig. 1) it was possible to follow individual MTs up to the distance of 30  $\mu\text{m}$  from the cell margin. This distance was equal to 1/2–1/3rd of the whole lamellae.

Plus ends elongated and shortened and occasionally paused. The full description of three-state dynamic instability requires calculation of two rates and six transition frequencies (growth to pause, growth to shortening, shortening to growth, shortening to pause, pause to shortening, and pause to growth). The growth rate in control cells was  $6.8 \pm 3.8 \mu\text{m}/\text{min}$  and the shortening rate was  $17.9 \pm 12.4 \mu\text{m}/\text{min}$ . Transition frequencies are presented in Table I.

Stabilization of the plus ends after nocodazole treatment resulted from the slight decrease of growth and shortening rates (to  $4.5 \pm 2.3 \mu\text{m}/\text{min}$  and  $15.2 \pm 8.1 \mu\text{m}/\text{min}$ , respectively) and a change in transition frequencies. Growth to pause and shortening to pause frequencies increased, while growth to shortening and shortening to growth frequencies decreased (Table I).

After inhibition of either Cdc42 or Rac1, growth and shortening rates did not change (Table I). Inhibition of either GTPase decreased the frequency of transition

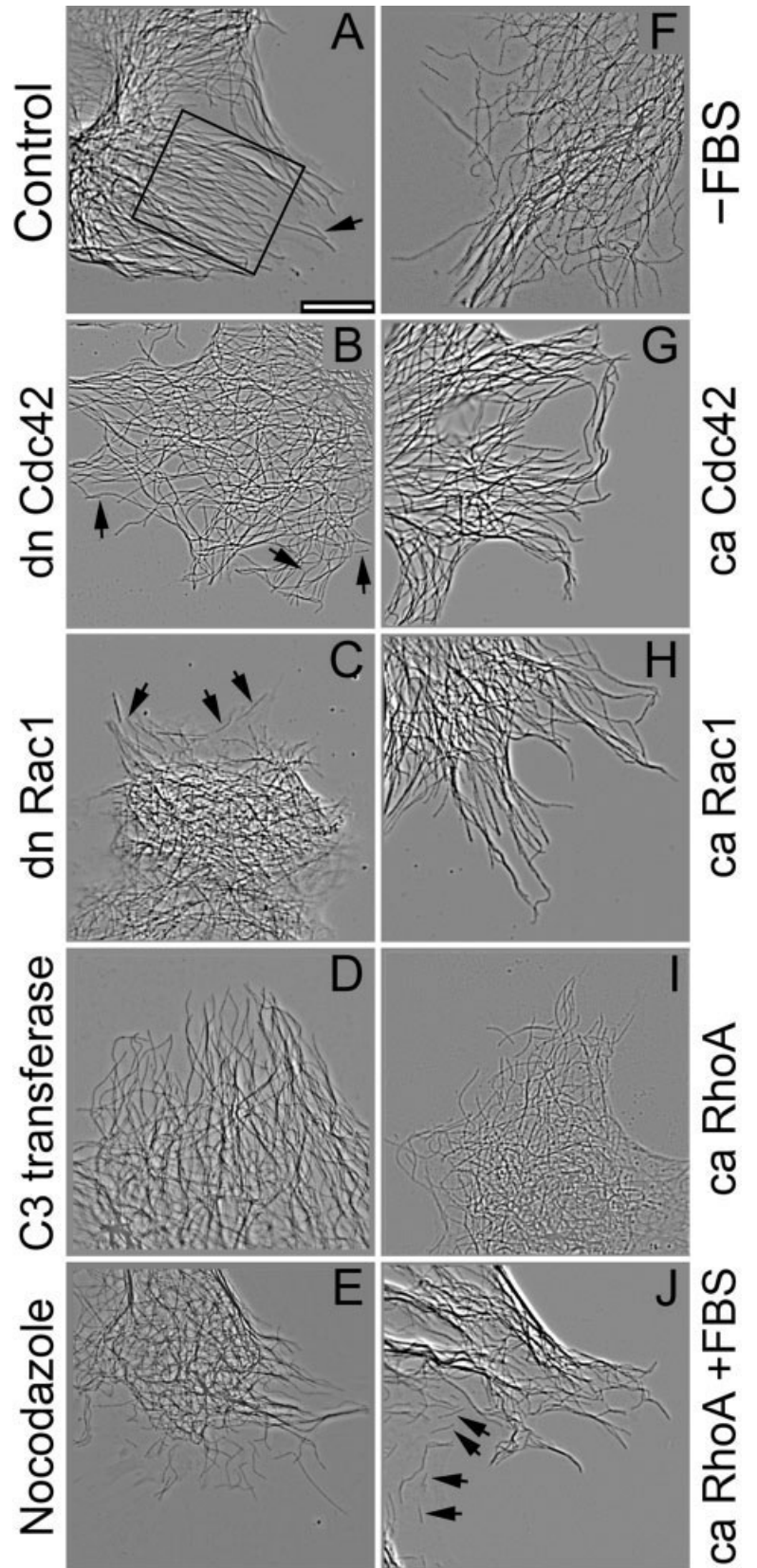


Fig. 1. Effects of Rho-GTPases inactivation and activation on the MT network. Live images of MTs in lamellae of Swiss 3T3 fibroblasts in a control cell(A), 30 min after microinjection of dominant negative Cdc42 protein into cells cultivated in full medium (B), 30 min after microinjection of dominant negative Rac1 protein into cells cultivated in full medium (C), 30 min after microinjection of C3-transferase into cells cultivated in full medium (D), 1 h after addition of 100 nM nocodazole (E), in lamellae of cells serum starved for 2 days (F), 30 min after microinjection of constitutively active Cdc42 protein into serum-starved cells (G), 30 min after microinjection of constitutively active Rac1 protein into serum-starved cells (H), 30 min after microinjection of constitutively active RhoA protein into serum-starved cells (I), 30 min after microinjection of constitutively active RhoA protein into cells cultivated in full medium (J). Free MTs are indicated by arrows. In (A) square box outlines the region of lamella where we analyzed the MT dynamics. We defined lamellae in accordance to Cramer et al. (1997) as flat anterior regions of polarized cells in front of the nucleus. Bar, 10 µm.

**TABLE I. Parameters of the Dynamic Instability of the Plus Ends in the Interior Region of the Lamella**

Parameter	Control	Nocodazole (100 nM)	Dominant negative Cdc42	Dominant negative Rac1
Growth rate ( $\mu\text{m}/\text{min}$ )	$6.8 \pm 3.8$	$4.5 \pm 2.3$	$6.5 \pm 3.8$	$5.7 \pm 2.4$
Shortening rate ( $\mu\text{m}/\text{min}$ )	$17.9 \pm 12.4$	$15.2 \pm 8.1$	$17.8 \pm 13.4$	$16.8 \pm 11.8$
Time spent in pause (%)	27	53	26	33
F growth to shortening ( $\text{min}^{-1}$ )	1.4	0.5	1.3	1.2
F growth to pause ( $\text{min}^{-1}$ )	1.2	2.2	1.1	1.3
F shortening to growth ( $\text{min}^{-1}$ )	5.7	3.7	5.5	4.6
F shortening to pause ( $\text{min}^{-1}$ )	0.6	3.9	0.7	1.5
F pause to shortening ( $\text{min}^{-1}$ )	0.9	1.3	1.6	1.1
F pause to growth ( $\text{min}^{-1}$ )	2.1	0.9	1.4	1.6
Total number of analyzed MTs/ number of cells	50/12	20/7	20/7	20/7

Parameters of the dynamic instability of the plus ends are presented as mean  $\pm$  SD for rates. Transitions frequencies are presented as a single value. F is frequency of transition between phases.

**TABLE II. Drift and Diffusion of the Plus Ends in the Interior Region of the Lamella**

Treatment	Serum	Drift ( $\mu\text{m}/\text{min}$ ; mean $\pm$ SEM)	Total number of MTs/ number of cells	Diffusion ( $\mu\text{m}^2/\text{min}$ ; mean $\pm$ SEM)	No. of MTs/ no. of cells
<i>Control</i>	+	$2.9 \pm 0.05$	1264/14	$19.6 \pm 1.2$	109/17
–FBS	–	$0.4 \pm 0.04^*$	1709/20	$7.7 \pm 0.8^{**}$	95/11
dn Cdc42	+	$0.8 \pm 0.04^*$	1085/12	$6.3 \pm 0.6^{**}$	156/7
dn Rac1	+	$-0.1 \pm 0.06^*$	1236/17	$2.6 \pm 0.3^{**}$	123/7
ca Cdc42	–	$2.5 \pm 0.03$	963/9	$16.8 \pm 0.8$	113/7
ca Rac1	–	$2.2 \pm 0.04$	1264/14	$17.2 \pm 0.9$	120/13
C3 transf.	+	$2.9 \pm 0.04$	1302/17	$17.3 \pm 1.6$	93/11
ca RhoA	–	$0.2 \pm 0.03^*$	1063/13	$6.9 \pm 0.6^{**}$	81/7
ca RhoA	+	$2.4 \pm 0.04$	902/11	$9.2 \pm 0.7^{**}$	107/13
Nocodazole (100 nM)	+	$0.2 \pm 0.05^*$	1063/13	$2.4 \pm 0.3^{**}$	97/11

Drift and diffusion coefficients for the plus ends are presented as a mean  $\pm$  SD. Abbreviations: –FBS, serum starvation; dn Cdc42, dominant negative Cdc42; dn Rac1, dominant negative Rac1; ca Cdc42, constitutively active Cdc42; ca Rac1, constitutively active Rac1; C3 transf., C3-transferase; caRhoA, constitutively active RhoA.

\*Indicates values of drift significantly smaller than those in the control cell ( $P < 0.01$ ).

\*\*Indicates values of diffusion significantly smaller than those in the control cells ( $P < 0.01$ ).

from pause to growth and increased the frequency of transition from pause to shortening (Table I). Thus exit from pauses, which was predominantly into growth in control cells (what could be considered as a rescue) turned to be redistributed randomly (into shortening and into growth) after Cdc42/Rac1 inactivation. Inhibition of Rac1 also altered the frequencies of exits from shortening (Table I). If in control cells shortening changed into growth more frequently than into pauses (what could also be considered as a prevalence of rescue), then after Rac1 inactivation exits from shortening were distributed more randomly (Table I).

The major changes in the parameters of dynamic instability observed after inactivation of Cdc42 or Rac1 or after incubation with nocodazole were in transition frequencies rather than in growth and shortening rates. However, to evaluate quantitatively the difference between MTs plus end behavior in the control cells and after inhibition of Cdc42 or Rac1 dynamic instability approach appeared to be inadequate. Thus, to quantify this effect we further used random walk approach [Vorobjev et al, 1997, 1999], which describes

dynamic instability in the steady state conditions [Maly, 2002].

### Inactivation of Cdc42 and Rac1 Stabilizes MT Plus Ends

In 3T3 fibroblasts polarized at the edge of an experimental wound the diffusion coefficient of MT plus ends was  $19.6 \pm 1.2 \mu\text{m}^2/\text{min}$  and the drift coefficient was  $2.9 \pm 0.05 \mu\text{m}/\text{min}$ . In serum depleted cells MT end diffusion coefficient was reduced to  $7.7 \pm 0.8 \mu\text{m}^2/\text{min}$ , and drift became negligible ( $0.4 \pm 0.04 \mu\text{m}/\text{min}$ ). Microinjection of either dominant negative Cdc42 or Rac1 had the same effect as serum depletion (Table II). The effect of dominant negative Rac1 was more profound than serum depletion (in agreement with the more profound effect of Rac1 on transition frequencies). In terms of diffusion with drift stabilization of MTs upon inactivation of Rac1 was almost the same as upon incubation of cells with nocodazole (Table II). In all cases random oscillations of the plus ends (i.e. traveled space) were decreased, and balance between growth and shortening in the internal cytoplasm was achieved.

### Activation of Cdc42 and Rac1 in Serum-Starved Cells Restores the Dynamics of MT Plus Ends

When cells incubated without serum for 2 days were microinjected with constitutively active Cdc42 or constitutively active Rac1 the diffusion coefficients for the plus ends of MTs increased and became close to that in control cells (Table II). The positive drift was also restored and its value became close to the control one. Within 30 min upon microinjection of either constitutively active protein, MTs in the lamellae became straight and ran perpendicularly to the cell edge (data not shown). Remarkably the difference between the effects of the two proteins was minor and statistically insignificant. Thus activation of either Cdc42 or Rac1 is sufficient to bring dynamics of the plus ends to the control state.

### RhoA Affects MT Dynamics Oppositely to Cdc42 and Rac1

Inhibition of RhoA with C3-transferase in normal cells had no effect on the dynamics of the plus ends (Table II). Microinjection of the constitutively active RhoA into serum-starved cells had no effect on diffusion and drift coefficients of the plus ends (compared with serum-starved cells) (Table II). Activation of RhoA in the cells grown in the full culture medium lead to unique effect—diffusion coefficient was reduced, yet drift coefficient hardly changed (Table II). Thus RhoA protein reduced random oscillations of the plus ends, but did not change the growth/shortening balance of them, allowing MTs to expand into new cytoplasmic protrusions.

The effects of the Rho proteins on the plus end dynamics might be summarized as follows: inhibition of Cdc42 or Rac1 as well as stimulation of RhoA reduces the dynamicity of the MT plus ends. Besides, inhibition of Cdc42 or Rac1 abrogates tendency for persistent growth of the plus ends. The next question we addressed was what happens to the MT minus ends under the same treatments?

### Regulation of the Minus End Dynamics by Rho Proteins

In a normal cell polarized at the edge of an experimental wound it was possible to observe 2–10 free MTs within 5 min (Fig. 1A). Free MTs were usually oriented along the cell axis, with their plus end distal and the minus end proximal. In all cases the difference between the opposite ends of a free MT was evident: minus end was shortening or paused, while the plus end showed alterations between growth and shortening similar to that of a centrosomally attached MT. The minus ends became visible mostly because their shortening brought them out of the dense MT meshwork and free MTs depolymerized completely within 1–2 min (Fig. 2A, Suppl. Video Fig. 2).

Since we did not observe any de novo formation of free MTs at the cell periphery, these MT fragments probably appeared because of MT breakage or release in the central cell regions.

In the control cells we followed 43 free minus ends, which shortened with the instantaneous rate of  $8.4 \pm 6.4 \mu\text{m}/\text{min}$ . Periods of depolymerization were interrupted by pauses (Fig. 2D). Pauses were not very long and majority of them (92.5%) did not exceed 1 min (Table III). However, some pauses reached 200–300 s and the histogram of duration of pauses was asymmetric (Fig. 2E). The mean rate of minus end shortening (calculated as the whole traveled distance divided to the whole time of observation, including pauses) was  $7.4 \pm 0.7 \mu\text{m}/\text{min}$  ( $\pm$ SEM).

After microinjection of either dominant-negative Cdc42 or Rac1 the number of free MTs increased and many of them did not show radial orientation (Figs. 1B and 1C). Since de novo formation of free MTs had not been observed, we assumed that inactivation of Cdc42 or Rac1 induced stabilization of the minus ends, which in turn resulted in longer lifespan of free MTs. Longer lifespan of free MTs is sufficient to increase their number. Indeed minus ends of free MTs after inactivation of either Cdc42 or Rac1 were found to continue to shorten with pauses but duration of pauses increased (Table III). Therefore the mean rate of shortening decreased, although the instantaneous rate of shortening was almost unchanged (Table III). Some free MTs became stable and survived through the whole time-lapse series (Figs. 2B and 2C, Suppl. Video Fig. 3). Typical life histories are shown in Fig. 2D. Stability of minus ends correlated with the increase of the average duration of pauses and the percentage of time spent in pauses (Figs. 2E and 2G). Average duration of pauses increased because pauses exceeding 1–2 min became much more frequent (Fig. 2E). It should be noted that in contrast to change in pause duration of the minus ends we observed no alterations in distribution of pause durations of the plus ends after Cdc42/Rac1 inactivation (Fig. 2F).

The behavior of the minus ends in serum-starved cells was similar to that after inactivation of either Cdc42 or Rac1 (Figs. 2D and 2G, Table III). Activation of either Cdc42 or Rac1 restored minus ends behavior to the control state (Figs. 2D and 2G, Table III).

Inactivation of RhoA in contrast to inactivation of Cdc42 and Rac1 did not stabilize the minus ends (Figs. 2D and 2G, Table III). Moreover, there was a tendency for a decrease in pause duration and an increase in the mean shortening rate (Table III). Activation of RhoA in serum-starved cells stabilized the minus ends (Figs. 2D and 2G, Table III). Activation of RhoA in the cells grown in complete medium not only increased the number of free MTs (Fig. 1J) but had an unique effect on the



TABLE III. Dynamics of the MT Minus Ends

	Serum	Total number of MTs/ number of cells	Drift ( $\mu\text{m}/\text{min}$ ; mean $\pm$ SEM)	Shortening		
				Instantaneous rate ( $\mu\text{m}/\text{min}$ )	Duration (s)	Pauses (duration; s)
Control	+	43/8	7.4 $\pm$ 0.7	8.4 $\pm$ 6.4	37.4 $\pm$ 33.2	29.8 $\pm$ 58.0
-FBS	-	50/13	3.8 $\pm$ 0.9*	11.9 $\pm$ 6.5	19.3 $\pm$ 16.8	43.4 $\pm$ 59.4
dn Cdc42	+	40/11	4.1 $\pm$ 0.8*	11.3 $\pm$ 6.5	25.1 $\pm$ 16.8	87.7 $\pm$ 92.9**
dn Rac1	+	36/12	3.2 $\pm$ 0.8*	10.0 $\pm$ 8.1	18.9 $\pm$ 12.9	55.6 $\pm$ 41.9**
ca Cdc42	-	39/7	8.2 $\pm$ 0.8	11.0 $\pm$ 5.7	21.7 $\pm$ 15.7	17.7 $\pm$ 16.5
ca Rac1	-	38/8	7.8 $\pm$ 0.9	11.1 $\pm$ 5.3	19.0 $\pm$ 12.4	22.5 $\pm$ 20.3
C3 transf	+	19/9	10.9 $\pm$ 1.9	14.8 $\pm$ 9.0	15.1 $\pm$ 15.1	18.2 $\pm$ 16.2
ca RhoA	-	19/7	3.1 $\pm$ 0.9*	10.0 $\pm$ 6.3	12.5 $\pm$ 10.7	35.9 $\pm$ 32.1
ca RhoA	+	30/9	2.5 $\pm$ 0.7*	9.0 $\pm$ 4.9	28.7 $\pm$ 33.5	113.0 $\pm$ 100.7**
Nocodazole	+	40/10	3.7 $\pm$ 0.8*	6.1 $\pm$ 3.4	20.2 $\pm$ 16.7	50.9 $\pm$ 66.7

Abbreviations: -FBS, serum starvation; dn Cdc42, dominant negative Cdc42; dn Rac1, dominant negative Rac1; ca Cdc42, constitutively active Cdc42; ca Rac1, constitutively active Rac1; C3 transf., C3-transferase; caRhoA, constitutively active RhoA.

\*Indicates values of drift significantly smaller than those in control cells ( $P < 0.01$ ).

\*\*Indicates pauses significantly longer than those in control cells ( $P < 0.05$ ).

behavior of such free MTs: their minus ends were stabilized and the mean rate of their shortening became close to the rate of the drift of the plus ends. This resulted in the elevation of the percentage of free MTs and in effective treadmilling of some of them (Suppl. Video Fig. 4).

## DISCUSSION

### Effects of Serum and Active RhoA on MT Stabilization

MT stabilization (an increase of MT lifespan), which can be easily detected because stable MTs accumulate posttranslational modifications (such as acetylated or detyrosinated tubulin), is the result of a lack of net depolymerization from both ends (we exclude the case of treadmilling because such "stable" MT will not accumulate posttranslational modification and will always travel through the lamella up to the cell border where they will depolymerize). Generation of stable MTs requires either capturing of their plus ends, accompanied by their paused state (which usually occurs at the cell cortex) or suppression of MT dynamics, resulting in short balanced polymerization and depolymerization episodes. In our analysis we focused on MTs that make no contact with the cell margin. Therefore, we did not consider the cell boundary effect [Komarova et al., 2002a], capturing of MT tips by the cell cortex [Mimori-Kiyosue et al., 2005] or by focal adhesions [Kaverina et al., 1998, 1999, 2000]. The internal (central) half of the lamella, where only processive growth is happening [Komarova et al., 2002a], was not analyzed either. In the peripheral half of the 3T3 fibroblast lamella, MT ends always displayed the alternation of growth, shortening and pauses and only at the cell cortex MTs could be observed to pause during the whole period of observation (5 min)

(data not shown). Free plus ends could (1) alternate between long growth and shrinking phases (as observed in control serum-grown cells) or (2) alternate between short growth and shrinking phases (as observed after serum depletion). The latter situation, which can be described as suppression of MT dynamics, would be expected to result in more stable MTs. Our data are in agreement with previously published study, which demonstrated that serum starvation inhibited dynamic instability, and after serum stimulation, MT dynamics was restored to control levels [Danowski, 1998]. This analysis is, however, at odds with another series of papers, which showed that the addition of LPA (one of the major active components of serum) to serum-depleted cells suppresses plus end dynamics [Nagasaki and Gundersen, 1996; Cook et al., 1998]. Formally, this contradiction could be explained by different cells used for that studies, NIH-3T3 [Cook et al., 1998] and Swiss 3T3 [Danowski, 1998; our study]. Also, in the previously published papers MT dynamics was analyzed at the periphery of the cell, but cortically captured and internal MTs were analyzed as one pool. Our recent observations [Mimori-Kiyosue et al., 2005] demonstrated that cortically located MT ends can have different dynamic properties from the ones located in the cell interior, and therefore, need to be analyzed as a different population.

It was previously shown that serum addition induced generation of stabilized, detyrosinated MT arrays [Gundersen et al., 1994]. It was further demonstrated that a certain component of serum, namely LPA, activates RhoA, which is responsible for MT stabilization [Nagasaki and Gundersen, 1996; Cook et al., 1998]. However, on our hands activation of RhoA in serum-starved cells as well as inactivation of RhoA in serum-grown cells had no strong effects on the dynamics of MT plus ends in internal cell regions in terms of diffusion with drift

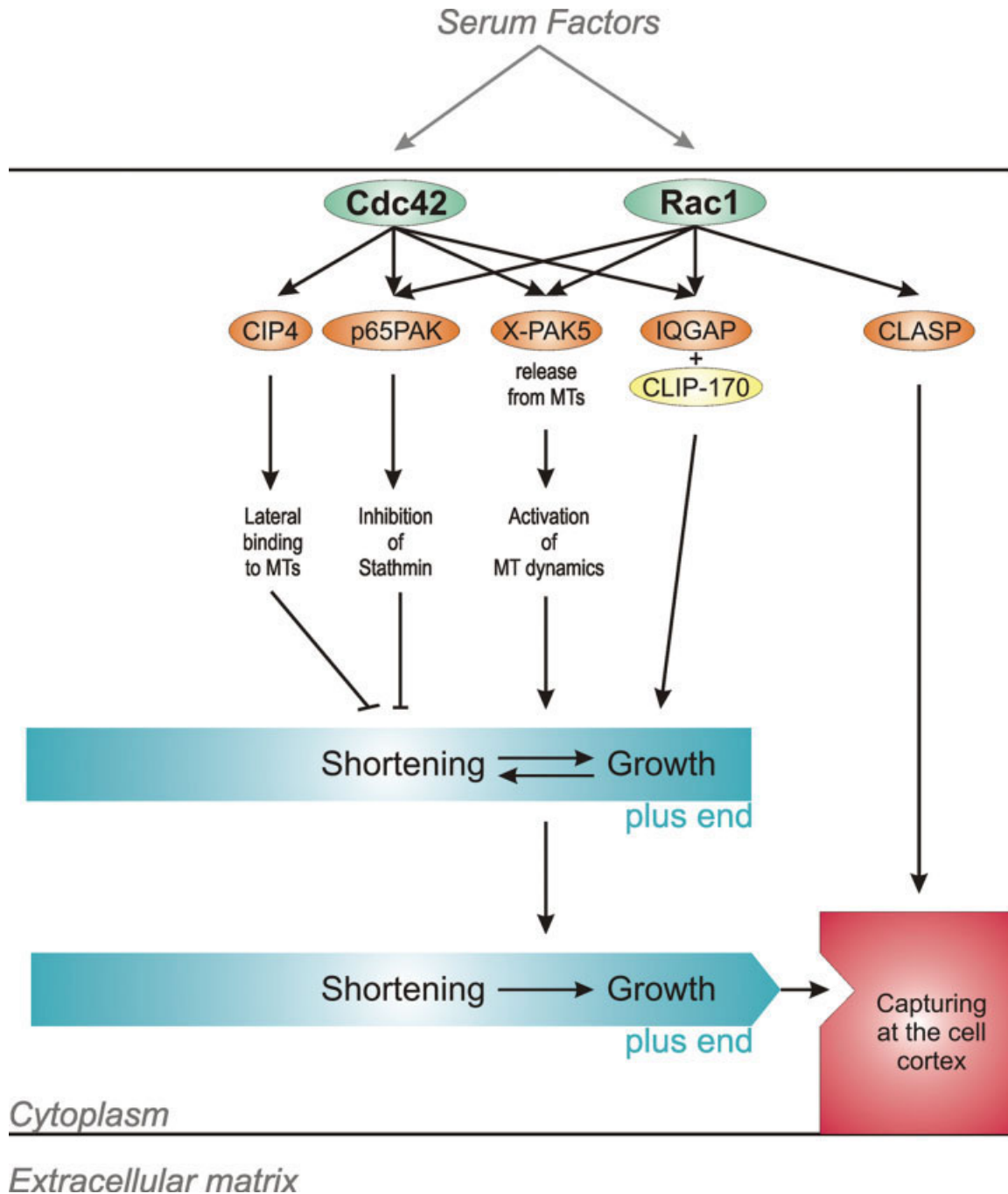


Fig. 3. The scheme of regulation of MT plus ends by Cdc42 and Rac1. Here we summarize the data on the known molecular interactions of Cdc42 and Rac1 downstream effectors with MTs and their possible implications for MT dynamics. The RhoA pathway had been extensively discussed elsewhere [Wen et al., 2004] and thus is not reviewed here.

comparing with serum-starved and serum-grown cells, respectively. This apparent contradiction can be best explained by proposing that the main activity of RhoA on MTs is through capturing and stabilization of their plus ends at the cell cortex and not on regulation of their dynamics in internal cell regions.

Activation of RhoA in the presence of serum resulted in suppression of minus end shortening and in reduced oscillations of the plus ends. Both effects enhance MT stability and may explain the generation of long-lived MTs, which can accumulate posttranslational modifications [Cook et al., 1998; Palazzo et al., 2001;

Wen et al., 2004]. Enhanced stability of MT also could be the reason for accumulation of curled MT, “wave-compressed” under the tension increased by RhoA activation. In control cells curled MT that could be generated by constriction of the part of the cell lamella would be quickly eliminated because of a higher rate of MT turnover. It should be noted that although both RhoA activation and Cdc42/Rac1 inactivation (or serum depletion) suppressed MT dynamics, in the first case growth still predominated over shortening, while in the second case polymerization/depolymerisation excursions in the internal cytoplasm were balanced. Predomination of growth is likely to be important for migrating cells for filling up the protruding lamella with new MTs (see below).

### Active Cdc42 and Rac1 Stimulate Plus End Rescue and Promote Minus End Depolymerization

Our study contributes quantitative data to the knowledge of action of Cdc42 and Rac1 on the MT dynamics in the internal cytoplasm. We found that both Cdc42 and Rac1 promote plus end rescue, stimulating transitions into growth and thereby shifting the imbalance of growth and shortening into growth. This observation is definitely in line with previous studies, such as the investigation of the behavior of pioneering MTs at the leading edge of PtK1 cells [Wittmann et al., 2003]. Several Cdc42 and Rac1 effectors could potentially achieve this effect. Cdc42 effector CIP4 binds laterally to MTs and can mediate the association of WASP with MTs [Tian et al., 2000]. This could stabilize MTs against shortening like MAP proteins do. Cdc42 and Rac1 mediate specific phosphorylation of stathmin via serine/threonine kinase p65PAK [Daub et al., 2001]. Stathmin is known as a MT destabilizing agent and its phosphorylation induced by Cdc42 and Rac1 inhibits its MT destabilizing activity. Cdc42/Rac effector X-PAK5 binds to MTs [Cau et al., 2001] and promotes the association of MTs into bundles similar to taxol. X-PAK5 also suppresses MT dynamics, slowing down both growth and shortening rates and inducing long pauses [Cau et al., 2001]. However, activation of Cdc42 or Rac1 displaces X-PAK5 from MTs to actin and promotes MT dynamics. Another effector of Rac1 and Cdc42, IQGAP1, was found to interact with CLIP-170 [Fukata et al., 2002], forming a tripartite complex. This complex localizes at cell cortex and was proposed to be a regulator of MT dynamics because it was shown that CLIP-170 is a MT rescue factor [Komarova et al., 2002b]. At the cell cortex, another +TIP, CLASP, which is regulated by Rac1, may be involved in MT capturing [Wittmann and Waterman-Storer, 2005]. The

data discussed above are summarized in a scheme presented in Fig. 3.

Besides the plus ends we have also analyzed the minus end dynamics when Cdc42 and Rac1 were either activated or inactivated. This analysis is novel because only a few studies addressed the minus end dynamics and none of them investigated the effect of Rho-GTPases. Analysis of minus end dynamics showed that again Cdc42 and Rac1 acted similarly, promoting minus end shortening. Taken together, our data show that Cdc42 and Rac1 stimulate plus end rescue that could be important for filling up freshly formed cell protrusions (which are also induced by Cdc42 and Rac1). In addition, they increase the MT turnover, promoting minus end depolymerization, which could contribute to the rapid MT network remodeling during cell locomotion. Both Cdc42 and Rac1 act on MT dynamics in a similar way, but the effects of Rac1 are somewhat stronger (Table II).

### CONCLUSIONS

In this study, we show that Cdc42 and Rac1 promote growth of free MT plus ends and stimulate MT minus end turnover. RhoA protein acts oppositely by suppressing the dynamics of both ends. We suggest that the regulation of MT dynamics by Rho proteins might be assumed as a basis of local MT regulation during cell locomotion and polarization. The exact pathways of this regulation remain to be investigated.

### ACKNOWLEDGMENTS

We thank Dr. A. Akhmanova for helpful discussion.

### REFERENCES

- Berg HC. 1993. *Random Walks in Biology*. Princeton: Princeton University Press. 287 p.
- Bergmann JE, Kupfer A, Singer SJ. 1983. Membrane insertion at the leading edge of motile fibroblasts. *Proc Natl Acad Sci USA* 80: 1367–1371.
- Cau J, Faure S, Comps M, Delsert C, Morin N. 2001. A novel p21-activated kinase binds the actin and microtubule networks and induces microtubule stabilization. *J Cell Biol* 155:1029–1042.
- Chausovsky A, Bershadsky AD, Borisy GG. 2000. Cadherin-mediated regulation of microtubule dynamics. *Nat Cell Biol* 2:797–804.
- Cook TA, Nagasaki T, Gundersen GG. 1998. Rho guanosine triphosphate mediates the selective stabilization of microtubules induced by lysophosphatidic acid. *J Cell Biol* 141:175–185.
- Cramer LP, Siebert M, Mitchison TJ. 1997. Identification of novel graded polarity actin filament bundles in locomoting heart fibroblasts: implications for the generation of motile force. *J Cell Biol* 136:1287–1305.
- Danowski BA. 1998. Microtubule dynamics in serum-starved and serum-stimulated Swiss 3T3 mouse fibroblasts: implications for the relationship between serum-induced contractility and microtubules. *Cell Motil Cytoskel* 40:1–12.

- Daub H, Gevaert K, Vandekerckhove J, Sobel A, Hall A. 2001. Rac/Cdc42 and p65PAK regulate the microtubule-destabilizing protein stathmin through phosphorylation at serine 16. *J Biol Chem* 276:1677–1680.
- Desai A, Mitchison TJ. 1997. Microtubule polymerization dynamics. *Annu Rev Cell Dev Biol* 13:83–117.
- Fukata M, Watanabe T, Noritake J, Nakagawa M, Yamaga M, Kuroda S, Matsuura Y, Iwamatsu A, Perez F, Kaibuchi K. 2002. Rac1 and Cdc42 capture microtubules through IQGAP1 and CLIP-170. *Cell* 109:873–885.
- Grigoriev IS, Chernobelskaya AA, Vorobjev IA. 1999. Nocodazole, vinblastine and taxol at low concentrations affect fibroblast locomotion and saltatory movements of organelles. *Membr Cell Biol* 13:23–48.
- Gundersen GG, Kim I, Chapin CJ. 1994. Induction of stable microtubules in 3T3 fibroblasts by TGF- $\beta$  and serum. *J Cell Sci* 107:645–659.
- Hirschberg K, Miller CM, Ellenberg J, Presley JF, Siggia ED, Phair RD, Lippincott-Schwartz J. 1998. Kinetic analysis of secretory protein traffic and characterization of golgi to plasma membrane transport intermediates in living cells. *J Cell Biol* 143:1485–1503.
- Kaverina I, Rottner K, Small JV. 1998. Targeting, capture, and stabilization of microtubules at early focal adhesions. *J Cell Biol* 142:181–190.
- Kaverina I, Krylyshkina O, Small JV. 1999. Microtubule targeting of substrate contacts promotes their relaxation and dissociation. *J Cell Biol* 146:1033–1044.
- Kaverina I, Krylyshkina O, Gimona M, Beningo K, Wang YL, Small JV. 2000. Enforced polarisation and locomotion of fibroblasts lacking microtubules. *Curr Biol* 10:739–742.
- Keating TJ, Peloquin JG, Rodionov VI, Momcilovic D, Borisy GG. 1997. Microtubule release from the centrosome. *Proc Natl Acad Sci USA* 94:5078–5083.
- Komarova YA, Vorobjev IA, Borisy GG. 2002a. Life cycle of MTs: persistent growth in the cell interior, asymmetric transition frequencies and effects of the cell boundary. *J Cell Sci* 115:3527–3539.
- Komarova YA, Akhmanova AS, Kojima S, Galjart N, Borisy GG. 2002b. Cytoplasmic linker proteins promote microtubule rescue in vivo. *J Cell Biol* 159:589–599.
- Kozma R, Ahmed S, Best A, Lim L. 1995. The Ras-related protein Cdc42Hs and bradykinin promote formation of peripheral actin microspikes and filopodia in Swiss 3T3 fibroblasts. *Mol Cell Biol* 15:1942–1952.
- Liao G, Nagasaki T, Gundersen GG. 1995. Low concentrations of nocodazole interfere with fibroblast locomotion without significantly affecting microtubule level: implications for the role of dynamic microtubules in cell locomotion. *J Cell Sci* 108:3473–3483.
- Lippincott-Schwartz J, Roberts TH, Hirschberg K. 2000. Secretory protein trafficking and organelle dynamics in living cells. *Annu Rev Cell Dev Biol* 16:557–589.
- Liu BP, Chrzanoska-Wodnicka M, Burridge K. 1998. Microtubule depolymerization induces stress fibers, focal adhesions, and DNA synthesis via the GTP-binding protein Rho. *Cell Adhes Commun* 5:249–255.
- Maly IV. 2002. Diffusion approximation of the stochastic process of microtubule assembly. *Bull Math Biol* 64:213–238.
- Mikhailov AV, Gundersen GG. 1995. Centripetal transport of microtubules in motile cells. *Cell Motil Cytoskel* 32:173–186.
- Mikhailov AV, Gundersen GG. 1998. Relationship between microtubule dynamics and lamellipodium formation revealed by direct imaging of microtubules in cells treated with nocodazole or taxol. *Cell Motil. Cytoskel.* 41:325–340.
- Mimori-Kiyosue Y, Grigoriev I, Lansbergen G, Sasaki H, Matsui C, Severin F, Galjart N, Grosveld F, Vorobjev I, Tsukita S, Akhmanova A. 2005. CLASP1 and CLASP2 bind to EB1 and regulate microtubule plus-end dynamics at the cell cortex. *J Cell Biol* 168:141–153.
- Nagasaki T, Gundersen GG. 1996. Depletion of lysophosphatidic acid triggers a loss of oriented detyrosinated microtubules in motile fibroblasts. *J Cell Sci* 109:2461–2469.
- Nobes CD, Hall A. 1995. Rho, rac, and cdc42 GTPases regulate the assembly of multimolecular focal complexes associated with actin stress fibers, lamellipodia, and filopodia. *Cell* 81:53–62.
- Nobes CD, Hall A. 1999. Rho GTPases control polarity, protrusion, and adhesion during cell movement. *J Cell Biol* 144:1235–1244.
- Palazzo AF, Cook TA, Alberts AS, Gundersen GG. 2001. mDia mediates Rho-regulated formation and orientation of stable microtubules. *Nat Cell Biol* 3:723–729.
- Ridley AJ, Hall A. 1992. The small GTP-binding protein rho regulates the assembly of focal adhesions and actin stress fibers in response to growth factors. *Cell* 70:389–399.
- Ridley AJ, Paterson HF, Johnston CL, Diekmann D, Hall A. 1992. The small GTP-binding protein rac regulates growth factor-induced membrane ruffling. *Cell* 70:401–410.
- Schmoranzer J, Kreitzer G, Simon SM. 2003. Migrating fibroblasts perform polarized, microtubule-dependent exocytosis towards the leading edge. *J Cell Sci* 116:4513–4519.
- Sekine A, Fujiwara M, Narumiya S. 1989. Asparagine residue in the rho gene product is the modification site for botulinum ADP-ribosyltransferase. *J Biol Chem* 264:8602–8605.
- Shelden E, Wadsworth P. 1993. Observation and quantification of individual microtubule behavior in vivo: microtubule dynamics are cell-type specific. *J Cell Biol* 120:935–945.
- Tian L, Nelson DL, Stewart DM. 2000. Cdc42-interacting protein 4 mediates binding of the Wiskott–Aldrich syndrome protein to microtubules. *J Biol Chem* 275:7854–7861.
- Vorobjev IA, Svitkina TM, Borisy GG. 1997. Cytoplasmic assembly of microtubules in cultured cells. *J Cell Sci* 110:2635–2645.
- Vorobjev IA, Rodionov VI, Maly IV, Borisy GG. 1999. Contribution of plus and minus end pathways to microtubule turnover. *J Cell Sci* 112:2277–2289.
- Wacker I, Kaether C, Kromer A, Migala A, Almers W, Gerdes HH. 1997. Microtubule-dependent transport of secretory vesicles visualized in real time with a GFP-tagged secretory protein. *J Cell Sci* 110:1453–1463.
- Waterman-Storer CM, Worthylake RA, Liu BP, Burridge K, Salmon ED. 1999. Microtubule growth activates Rac1 to promote lamellipodial protrusion in fibroblasts. *Nat Cell Biol* 1:45–50.
- Wen Y, Eng CH, Schmoranzer J, Cabrera-Poch N, Morris EJ, Chen M, Wallar BJ, Alberts AS, Gundersen GG. 2004. EB1 and APC bind to mDia to stabilize microtubules downstream of Rho and promote cell migration. *Nat Cell Biol* 6:820–830.
- Wittmann T, Bokoch GM, Waterman-Storer CM. 2003. Regulation of leading edge microtubule and actin dynamics downstream of Rac1. *J Cell Biol* 161:845–851.
- Wittmann T, Waterman-Storer CM. 2005. Spatial regulation of CLASP affinity for microtubules by Rac1 and GSK3 $\beta$  in migrating epithelial cells. *J Cell Biol* 169:929–939.